SLAC–PUB–10812
October 2004

New Results in Light-Front Phenomenology*

Stanley J. Brodsky
Stanford Linear Accelerator Center
Stanford University, Stanford, California 94309
E-mail: sjbth@slac.stanford.edu

Presented at
LightCone 2004
Amsterdam, The Netherlands
16–20 August 2004

*Work supported by Department of Energy contract DE–AC02–76SF00515.

Abstract

The light-front quantization of gauge theories in light-cone gauge provides a frame-independent wavefunction representation of relativistic bound states, simple forms for current matrix elements, explicit unitarity, and a trivial vacuum. In this talk I review the theoretical methods and constraints which can be used to determine these central elements of QCD phenomenology. The freedom to choose the light-like quantization four-vector provides an explicitly covariant formulation of light-front quantization and can be used to determine the analytic structure of light-front wave functions and define a kinematical definition of angular momentum. The AdS/CFT correspondence of large N_C supergravity theory in higher-dimensional anti-de Sitter space with supersymmetric QCD in 4-dimensional space-time has interesting implications for hadron phenomenology in the conformal limit, including an all-orders demonstration of counting rules for exclusive processes. String/gauge duality also predicts the QCD power-law behavior of light-front Fock-state hadronic wavefunctions with arbitrary orbital angular momentum at high momentum transfer. The form of these near-conformal wavefunctions can be used as an initial ansatz for a variational treatment of the light-front QCD Hamiltonian. The light-front Fock-state wavefunctions encode the bound state properties of hadrons in terms of their quark and gluon degrees of freedom at the amplitude level. The nonperturbative Fock state wavefunctions contain intrinsic gluons, and sea quarks at any scale Q with asymmetries such as $s(x) \neq \bar{s}(x)$, $\bar{u}(x) \neq \bar{d}(x)$. Intrinsic charm and bottom quarks appear at large x in the light-front wavefunctions since this minimizes the invariant mass and off-shellness of the higher Fock state. In the case of nuclei, the Fock state expansion contains "hidden color" states which cannot be classified in terms of nucleonic degrees of freedom. I also briefly review recent analyses which shows that some leading-twist phenomena such as the diffractive component of deep inelastic scattering, single-spin asymmetries, nuclear shadowing and antishadowing cannot be computed from the LFWFs of hadrons in isolation.

1 Introduction

A central problem in nonperturbative quantum chromodynamics is to determine not only the masses but also the wavefunctions of hadronic bound states. Relativity and quantum mechanics requires that a hadron fluctuates not only in coordinate space, spin, and color, but also in the number of quanta. The light-front Hamiltonian formulation of quantum chromodynamics provides a comprehensive formulation for determining not only the spectrum of the theory, but also the complete set of light-front Fock state wavefunctions $\psi_{n/H}(x_i, \vec{k}_{\perp i}, \lambda_i)$ which encode the bound state properties of hadrons in terms of their fundamental quark and gluon degrees of freedom at the amplitude level.

Formally, the light-front expansion is constructed by quantizing QCD at fixed light-cone time [1] $\tau = t + z/c$ and forming the invariant light-front Hamiltonian: $H_{LF}^{QCD} = P^+P^- - \vec{P}_\perp^2$ where $P^\pm = P^0 \pm P^z$ [2]. The momentum generators P^+ and $\vec{P}_\perp$ are kinematical; *i.e.*, they are independent of the interactions. The generator $P^- = i\frac{d}{d\tau}$ generates light-cone time translations, and the eigen-spectrum of the Lorentz scalar H_{LF}^{QCD} gives the mass spectrum of the color-singlet hadron states in QCD together with their respective light-front wavefunctions. For example, the proton state satisfies: $H_{LF}^{QCD} \mid \psi_p\rangle = M_p^2 \mid \psi_p\rangle$.

The light-front (LF) quantization of QCD in light-cone gauge $A^+ = 0$ has a number of remarkable advantages, including explicit unitarity, a physical Fock expansion, the absence of ghost degrees of freedom, and the decoupling properties needed to prove factorization theorems in high momentum transfer inclusive and exclusive reactions. Prem Srivastava and I have given a systematic derivation [3] of LF-quantized gauge theory using the Dirac method of constraints. The free theory gauge field is shown to satisfy the Lorentz condition as an operator equation as well as the light-cone gauge condition. Its propagator is found to be transverse with respect to both its four-momentum and the gauge direction. The interaction Hamiltonian of QCD has a form resembling that of covariant theory, except for additional instantaneous interactions which can be treated systematically. The QCD β function computed in the light-cone gauge agrees with that known in the conventional framework. In the case of the electroweak theory, spontaneous symmetry breaking is realized in LF quantization by the appearance of zero modes of the Higgs field. Light-front quantization leads to an elegant ghost-free theory of massive gauge particles, automatically incorporating the Lorentz and 't Hooft conditions, as well as the Goldstone boson equivalence theorem [4].

The expansion of the proton eigensolution $\mid \psi_p\rangle$ on the color-singlet $B = 1$, $Q = 1$ eigenstates $\{\mid n\rangle\}$ of the free Hamiltonian $H_{LF}^{QCD}(g = 0)$ gives the light-front Fock expansion:

$$\Big\mid \psi_p(P^+, \vec{P}_\perp)\Big\rangle \;=\; \sum_n \prod_{i=1}^n \frac{\mathrm{d}x_i\, \mathrm{d}^2\vec{k}_{\perp i}}{\sqrt{x_i}\, 16\pi^3}\; 16\pi^3\; \delta\left(1 - \sum_{i=1}^n x_i\right)\; \delta^{(2)}\left(\sum_{i=1}^n \vec{k}_{\perp i}\right) \qquad (1)$$

$$\times \psi_{n/H}(x_i, \vec{k}_{\perp i}, \lambda_i) \left| n;\, x_i P^+, x_i \vec{P}_\perp + \vec{k}_{\perp i}, \lambda_i \right\rangle .$$

The light-cone momentum fractions $x_i = k_i^+/P^+$ and $\vec{k}_{\perp i}$ represent the relative momentum coordinates of the QCD constituents. The physical transverse momenta are $\vec{p}_{\perp i} = x_i \vec{P}_\perp + \vec{k}_{\perp i}$. The λ_i label the light-cone spin projections S^z of the quarks and gluons along the quantization direction z. Each Fock component has the invariant mass squared

$$\mathcal{M}_n^2 = (\sum_{i=1}^n k_i^\mu)^2 = \sum_{i=1}^n \frac{k_{\perp i}^2 + m_i^2}{x_i}. \tag{2}$$

The physical gluon polarization vectors $\epsilon^\mu(k,\, \lambda = \pm 1)$ are specified in light-cone gauge by the conditions $k \cdot \epsilon = 0,\ \eta \cdot \epsilon = \epsilon^+ = 0$. The gluonic quanta which appear in the Fock states thus have physical polarization $\lambda = \pm 1$ and positive metric. Since each Fock particle is on its mass shell in a Hamiltonian framework, $k^- = k^0 - k^z = \frac{k_\perp^2 + m^2}{k^+}$. One cannot truncate the LF expansion; the expansion sum runs over all n, beginning with the lowest valence state. The probability of massive Fock states with invariant mass $\mathcal{M}$ falls-off at least as fast as $1/\mathcal{M}^2$.

Because they are defined at fixed light-front time $\tau = t + z/c$ (Dirac's "Front Form"), LFWFs have the remarkable property of being independent of the hadron's four-momentum. In contrast, in equal-time quantization, a Lorentz boost mixes dynamically with the interactions, so that computing a wavefunction in a new frame at fixed t requires solving a nonperturbative problem as complicated as the Hamiltonian eigenvalue problem itself. The LFWFs are properties of the hadron itself; they are thus universal and process independent.

The light-front Fock state expansion provides important perspectives on the quark and gluon distributions of hadrons. For example, there is no scale Q_0 where one can limit the quark content of a hadron to valence quarks. The nonperturbative Fock state wavefunctions contain intrinsic gluons, strange quarks, charm quarks, etc., at any scale. The internal QCD interactions lead to asymmetries such as $s(x) \neq \bar{s}(x)$, $\bar{u}(x) \neq \bar{d}(x)$ and intrinsic charm and bottom distributions at large x since this minimizes the invariant mass and off-shellness of the higher Fock state. In the case of nuclei, the Fock state expansion contains hidden color states which cannot be classified in terms of nucleonic degrees of freedom. However, some leading-twist phenomena such as the diffractive component of deep inelastic scattering, single-spin asymmetries, nuclear shadowing and antishadowing cannot be computed from the LFWFs of hadrons in isolation. These issues are reviewed in Section 5 below.

One of the important aspects of fundamental hadron structure is the presence of non-zero orbital angular momentum in the bound-state wave functions. The evidence for a "spin crisis" in the Ellis-Jaffe sum rule signals a significant orbital contribution in the proton wave function [5, 6]. The Pauli form factor of nucleons is computed from the overlap of LFWFs differing by one unit of orbital angular momentum $\Delta L_z = \pm 1$. Thus the fact that the anomalous moment of the proton is non-zero requires nonzero

orbital angular momentum in the proton wavefunction [7]. In the light-front method, orbital angular momentum is treated explicitly; it includes the orbital contributions induced by relativistic effects, such as the spin-orbit effects normally associated with the conventional Dirac spinors. Angular momentum conservation for each Fock state implies

$$J^z = \sum_i^n S_i^z + \sum_i^{n-1} L_i^z \tag{3}$$

where L_i^z is one of the $n-1$ relative orbital angular momenta.

One can also define the light-front Fock expansion using a covariant generalization of light-front time: $\tau = x{\cdot}\omega$. The four-vector ω, with $\omega^2 = 0$, determines the orientation of the light-front plane; the freedom to choose ω provides an explicitly covariant formulation of light-front quantization [8]: all observables such as matrix elements of local current operators, form factors, and cross sections are light-front invariants – they must be independent of ω_μ. In recent work, Dae Sung Hwang, John Hiller, Volodya Karmonov [9], and I have studied the analytic structure of LFWFs using the explicitly Lorentz-invariant formulation of the front form. Eigensolutions of the Bethe-Salpeter equation have specific angular momentum as specified by the Pauli-Lubanski vector. The corresponding LFWF for an n-particle Fock state evaluated at equal light-front time $\tau = \omega \cdot x$ can be obtained by integrating the Bethe-Salpeter solutions over the corresponding relative light-front energies. The resulting LFWFs $\psi_n^I(x_i, k_{\perp i})$ are functions of the light-cone momentum fractions $x_i = k_i \cdot \omega / p \cdot \omega$ and the invariant mass of the constituents $\mathcal{M}_n$, each multiplying spin-vector and polarization tensor invariants which can involve ω^μ. They are eigenstates of the Karmanov–Smirnov kinematic angular momentum operator [10, 8].

$$\vec{J} = -i[\vec{k} \times \partial/\partial\vec{k}\,] - i[\vec{n} \times \partial/\partial\vec{n}] + \frac{1}{2}\vec{\sigma}, \tag{4}$$

where $\vec{n}$ is the spatial component of ω in the constituent rest frame ($\vec{\mathcal{P}} = \vec{0}$). Although this form is written specifically in the constituent rest frame, it can be generalized to an arbitrary frame by a Lorentz boost.

Normally the generators of angular rotations in the LF formalism contain interactions, as in the Pauli–Lubanski formulation; however, the LF angular momentum operator can also be represented in the kinematical form (4) without interactions. The key term is the generator of rotations of the LF plane $-i[\vec{n} \times \partial/\partial\vec{n}]$ which replaces the interaction term; it appears only in the explicitly covariant formulation, where the dependence on $\vec{n}$ is present. Thus LFWFs satisfy all Lorentz symmetries of the front form, including boost invariance, and they are proper eigenstates of angular momentum.

In principle, one can solve for the LFWFs directly from the fundamental theory using methods such as discretized light-front quantization (DLCQ) [11], the transverse lattice [12, 13, 14], lattice gauge theory moments [15], Dyson-Schwinger techniques [16], and Bethe–Salpeter techniques [9]. DLCQ has been remarkably success-

ful in determining the entire spectrum and corresponding LFWFs in one space-one time field theories [17], including QCD(1+1) [18] and SQCD(1+1) [19]. There are also DLCQ solutions for low sectors of Yukawa theory in physical space-time dimensions [20]. The DLCQ boundary conditions allow a truncation of the Fock space to finite dimensions while retaining the kinematic boost and Lorentz invariance of light-front quantization.

The transverse lattice method combines DLCQ for one-space and the light-front time dimensions with lattice theory in transverse space. It has recently provided the first computation of the generalized parton distributions of the pion [13]. Dyson-Schwinger methods account well for running quark mass effects, and in principle can give important hadronic wavefunction information. One can also project known solutions of the Bethe–Salpeter equation to equal light-front time, thus producing hadronic light-front Fock wave functions [9]. Bakker and van Iersel have developed new methods to find solutions to bound-state light-front equations in ladder approximation [21]. Pauli has shown how one can construct an effective light-front Hamiltonian which acts within the valence Fock state sector alone [22]. Another possible method is to construct the $q\bar{q}$ Green's function using light-front Hamiltonian theory, DLCQ boundary conditions and Lippmann-Schwinger resummation. The zeros of the resulting resolvent projected on states of specific angular momentum J_z can then generate the meson spectrum and their light-front Fock wavefunctions. As emphasized by Weinstein and Vary, new effective operator methods [23, 24] which have been developed for Hamiltonian theories in condensed matter and nuclear physics, could also be applied advantageously to light-front Hamiltonian. Reviews of nonperturbative light-front methods may be found in references [2, 8, 25, 26].

Even without explicit solutions, much is known about the explicit form and structure of LFWFs. They can be matched to nonrelativistic Schrodinger wavefunctions at soft scales. At high momenta, the LFWFs at large $k_\perp$ and $x_i \to 1$ are constrained by arguments based on conformal symmetry, the operator product expansion, or perturbative QCD. The pattern of higher Fock states with extra gluons is given by ladder relations [27]. The structure of Fock states with nonzero orbital angular momentum is also constrained by the Karmanov-Smirnov operator [10].

2 AdS/CFT and Its Consequences for Near-Conformal Field Theory

As shown by Maldacena [28], there is a remarkable correspondence between large N_C supergravity theory in a higher dimensional anti-de Sitter space and supersymmetric QCD in 4-dimensional space-time. String/gauge duality provides a framework for predicting QCD phenomena based on the conformal properties of the AdS/CFT correspondence. For example, Polchinski and Strassler [29] have shown that the power-law fall-off of hard exclusive hadron-hadron scattering amplitudes at large momentum

transfer can be derived without the use of perturbation theory by using the scaling properties of the hadronic interpolating fields in the large-r region of AdS space. Thus one can use the Maldacena correspondence to compute the leading power-law falloff of exclusive processes such as high-energy fixed-angle scattering of gluonium-gluonium scattering in supersymmetric QCD. The resulting predictions for hadron physics effectively coincide [29, 30, 31] with QCD dimensional counting rules [32, 33, 34, 35]. Polchinski and Strassler [29] have also derived counting rules for deep inelastic structure functions at $x \to 1$ in agreement with perturbative QCD predictions [36] as well as Bloom-Gilman exclusive-inclusive duality. An interesting point is that the hard scattering amplitudes which are normally or order α_s^p in PQCD appear as order $\alpha_s^{p/2}$ in the supergravity predictions. This can be understood as an all-orders resummation of the effective potential [28, 37]. The near-conformal scaling properties of light-front wavefunctions thus lead to a number of important predictions for QCD which are normally discussed in the context of perturbation theory.

De Teramond and I [38] have shown how one can use the scaling properties of the hadronic interpolating operator in the extended AdS/CFT space-time theory to determine the form of QCD wavefunctions at large transverse momentum $k_\perp^2 \to \infty$ and at $x \to 1$ [38]. The angular momentum dependence of the light-front wavefunctions also follow from the conformal properties of the AdS/CFT correspondence. The scaling and conformal properties of the correspondence leads to a hard component of the light-front Fock state wavefunctions of the form:

$$\psi_{n/h}(x_i, \vec{k}_{\perp i}, \lambda_i, l_{zi}) \;\sim\; \frac{(g_s\ N_C)^{\frac{1}{2}(n-1)}}{\sqrt{N_C}} \prod_{i=1}^{n-1} (k_{i\perp}^{\pm})^{|l_{zi}|} \times \left[\frac{\Lambda_o}{M^2 - \sum_i \frac{\vec{k}_{\perp i}^2 + m_i^2}{x_i} + \Lambda_o^2} \right]^{n+\sum_i |l_{zi}|-1}, \tag{5}$$

where g_s is the string scale and Λ_o represents the basic QCD mass scale. The scaling predictions agree with the perturbative QCD analysis given in the references [39], but the AdS/CFT analysis is performed at strong coupling without the use of perturbation theory. The form of these near-conformal wavefunctions can be used as an initial ansatz for a variational treatment of the light-front QCD Hamiltonian.

The recent investigations using the AdS/CFT correspondence has reawakened interest in the conformal features of QCD [40]. QCD becomes scale free and conformally symmetric in the analytic limit of zero quark mass and zero β function [41]. This correspondence principle provides a new tool, the conformal template, which is very useful for theory analyses, such as the expansion polynomials for distribution amplitudes [42, 43, 44, 45], the non-perturbative wavefunctions which control exclusive processes at leading twist [46, 47]. The near-conformal behavior of QCD is also the basis for commensurate scale relations [48] which relate observables to each other without renormalization scale or scheme ambiguities [49]. An important exam-

ple is the generalized Crewther relation [50]. In this method the effective charges of observables are related to each other in conformal gauge theory; the effects of the nonzero QCD $\beta-$ function are then taken into account using the BLM method [51] to set the scales of the respective couplings. The magnitude of the corresponding effective charge [52] $\alpha_s^{\rm exclusive}(Q^2) = F_\pi(Q^2)/4\pi Q^2 F^2_{\gamma\pi^0}(Q^2)$ for exclusive amplitudes is connected to the effective charge α_τ defined from τ hadronic decays [53] by a commensurate scale relation. Its magnitude: $\alpha_s^{\rm exclusive}(Q^2) \sim 0.8$ at small Q^2, is sufficiently large as to explain the observed magnitude of exclusive amplitudes such as the pion form factor using the asymptotic distribution amplitude [54].

Theoretical [55, 56, 57, 58, 59] and phenomenological [60, 53, 61] evidence is now accumulating that the QCD coupling becomes constant at small virtuality; *i.e.*, $\alpha_s(Q^2)$ develops an infrared fixed point in contradiction to the usual assumption of singular growth in the infrared. If QCD running couplings are bounded, the integration over the running coupling is finite and renormalon resummations are not required. If the QCD coupling becomes scale-invariant in the infrared, then elements of conformal theory [45] become relevant even at relatively small momentum transfers.

Menke, Merino, and Rathsman [53] and I have presented a definition of a physical coupling for QCD which has a direct relation to high precision measurements of the hadronic decay channels of the $\tau^- \to \nu_\tau {\rm H}^-$. Let R_τ be the ratio of the hadronic decay rate to the leptonic one. Then $R_\tau \equiv R_\tau^0 \left[1 + \frac{\alpha_\tau}{\pi}\right]$, where R_τ^0 is the zeroth order QCD prediction, defines the effective charge α_τ. The data for τ decays is well-understood channel by channel, thus allowing the calculation of the hadronic decay rate and the effective charge as a function of the τ mass below the physical mass. The vector and axial-vector decay modes can be studied separately. Using an analysis of the τ data from the OPAL collaboration [62], we have found that the experimental value of the coupling $\alpha_\tau(s) = 0.621 \pm 0.008$ at $s = m_\tau^2$ corresponds to a value of $\alpha_{\overline{\rm MS}}(M_Z^2) = (0.117$-$0.122) \pm 0.002$, where the range corresponds to three different perturbative methods used in analyzing the data. This result is in good agreement with the world average $\alpha_{\overline{\rm MS}}(M_Z^2) = 0.117 \pm 0.002$. However, one also finds that the effective charge only reaches $\alpha_\tau(s) \sim 0.9 \pm 0.1$ at $s = 1\,{\rm GeV}^2$, and it even stays within the same range down to $s \sim 0.5\,{\rm GeV}^2$. The effective coupling is close to constant at low scales, suggesting that physical QCD couplings become constant or "frozen" at low scales.

The near constancy of the effective QCD coupling at small scales helps explain the empirical success of dimensional counting rules for the power law fall-off of form factors and fixed angle scaling. As shown in the references [52, 63], one can calculate the hard scattering amplitude T_H for such processes [54] without scale ambiguity in terms of the effective charge α_τ or α_R using commensurate scale relations. The effective coupling is evaluated in the regime where the coupling is approximately constant, in contrast to the rapidly varying behavior from powers of $\alpha_{\rm s}$ predicted by perturbation theory (the universal two-loop coupling). For example, the nucleon form factors are proportional at leading order to two powers of $\alpha_{\rm s}$ evaluated at low scales in addition to two powers of $1/q^2$; The pion photoproduction amplitude at fixed

angles is proportional at leading order to three powers of the QCD coupling. The essential variation from leading-twist counting-rule behavior then only arises from the anomalous dimensions of the hadron distribution amplitudes.

3 Light-Front Phenomenology

Light-front Fock state wavefunctions $\psi_{n/H}(x_i, \vec{k}_{\perp i}, \lambda_i)$ play an essential role in QCD phenomenology, generalizing Schrödinger wavefunctions $\psi_H(\vec{k})$ of atomic physics to relativistic quantum field theory. Given the $\psi^{(\Lambda)}_{n/H}$, one can construct any spacelike electromagnetic, electroweak, or gravitational form factor or local operator product matrix element of a composite or elementary system from the diagonal overlap of the LFWFs [7]. Exclusive semi-leptonic B-decay amplitudes involving timelike currents such as $B \to A\ell\bar{\nu}$ can also be evaluated exactly in the light-front formalism [64]. In this case, the timelike decay matrix elements require the computation of both the diagonal matrix element $n \to n$ where parton number is conserved and the off-diagonal $n+1 \to n-1$ convolution such that the current operator annihilates a $q\bar{q}'$ pair in the initial B wavefunction. This term is a consequence of the fact that the time-like decay $q^2 = (p_\ell + p_{\bar{\nu}})^2 > 0$ requires a positive light-cone momentum fraction $q^+ > 0$. Conversely for space-like currents, one can choose $q^+ = 0$, as in the Drell-Yan-West representation of the space-like electromagnetic form factors. The light-front Fock representation thus provides an exact formulation of current matrix elements of local operators. In contrast, in equal-time Hamiltonian theory, one must evaluate connected time-ordered diagrams where the gauge particle or graviton couples to particles associated with vacuum fluctuations. Thus even if one knows the equal-time wavefunction for the initial and final hadron, one cannot determine the current matrix elements. In the case of the covariant Bethe-Salpeter formalism, the evaluation of the matrix element of the current requires the calculation of an infinite number of irreducible diagram contributions.

One can also prove directly from the LFWF overlap representation that the anomalous gravitomagnetic moment $B(0)$ vanishes for any composite system [65]. This property follows directly from the Lorentz boost properties of the light-front Fock representation and holds separately for each Fock state component.

Given the LFWFs, one can also compute the hadronic distribution amplitudes $\phi_H(x_i, Q)$ which control hard exclusive processes as an integral over the transverse momenta of the valence Fock state LFWFs [54]. In addition one can compute the unintegrated parton distributions in x and $k_\perp$ which underlie generalized parton distributions for nonzero skewness. As shown by Diehl, Hwang, and myself [66], one can give a complete representation of virtual Compton scattering $\gamma^* p \to \gamma p$ at large initial photon virtuality Q^2 and small momentum transfer squared t in terms of the light-cone wavefunctions of the target proton. One can then verify the identities between the skewed parton distributions $H(x, \zeta, t)$ and $E(x, \zeta, t)$ which appear in deeply

virtual Compton scattering and the corresponding integrands of the Dirac and Pauli form factors $F_1(t)$ and $F_2(t)$ and the gravitational form factors $A_q(t)$ and $B_q(t)$ for each quark and anti-quark constituent. We have illustrated the general formalism for the case of deeply virtual Compton scattering on the quantum fluctuations of a fermion in quantum electrodynamics at one loop.

The integrals of the unintegrated parton distributions over transverse momentum at zero skewness provide the helicity and transversity distributions measurable in polarized deep inelastic experiments [54]. For example, the polarized quark distributions at resolution Λ correspond to

$$\begin{aligned} q_{\lambda_q/\Lambda_p}(x,\Lambda) &= \sum_{n,q_a} \int \prod_{j=1}^{n} dx_j d^2k_{\perp j} \sum_{\lambda_i} |\psi^{(\Lambda)}_{n/H}(x_i,\vec{k}_{\perp i},\lambda_i)|^2 \\ &\times \delta\left(1-\sum_i^n x_i\right)\delta^{(2)}\left(\sum_i^n \vec{k}_{\perp i}\right)\delta(x-x_q) \\ &\times \delta_{\lambda_a,\lambda_q}\Theta(\Lambda^2-\mathcal{M}_n^2)\ , \end{aligned} \tag{6}$$

where the sum is over all quarks q_a which match the quantum numbers, light-cone momentum fraction x, and helicity of the struck quark.

Hadronization phenomena such as the coalescence mechanism for leading heavy hadron production are computed from LFWF overlaps. Diffractive jet production provides another phenomenological window into the structure of LFWFs. However, as shown recently [67], some leading-twist phenomena such as the diffractive component of deep inelastic scattering, single spin asymmetries, nuclear shadowing and antishadowing cannot be computed from the LFWFs of hadrons in isolation.

As shown by Raufeisen and myself [68], one can construct a "light-front density matrix" from the complete set of light-front wavefunctions which is a Lorentz scalar. This form can be used at finite temperature to give a boost invariant formulation of thermodynamics. At zero temperature the light-front density matrix is directly connected to the Green's function for quark propagation in the hadron as well as deeply virtual Compton scattering. One can also define a light-front partition function Z_{LF} as an outer product of light-front wavefunctions. The deeply virtual Compton amplitude and generalized parton distributions can then be computed as the trace $Tr[Z_{LF}\mathcal{O}]$, where $\mathcal{O}$ is the appropriate local operator [68]. This partition function formalism can be extended to multi-hadronic systems and systems in statistical equilibrium to provide a Lorentz-invariant description of relativistic thermodynamics [68].

4 Complications from Final-State Interactions

Although it has been more than 35 years since the discovery of Bjorken scaling [69] in electroproduction [70], there are still many issues in deep-inelastic lepton scattering and Drell-Yan reactions which are only now being understood from a fundamental

basis in QCD. In contrast to the parton model, final-state interactions in deep inelastic scattering and initial state interactions in hard inclusive reactions cannot be neglected—leading to $T-$odd single spin asymmetries [71, 72, 73] and diffractive contributions [67, 74]. This in turn implies that the structure functions measured in deep inelastic scattering are not probability distributions computed from the square of the LFWFs computed in isolation [67].

It is usually assumed—following the parton model—that the leading-twist structure functions measured in deep inelastic lepton-proton scattering are simply the probability distributions for finding quarks and gluons in the target nucleon. In fact, gluon exchange between the fast, outgoing quarks and the target spectators effects the leading-twist structure functions in a profound way, leading to diffractive leptoproduction processes, shadowing of nuclear structure functions, and target spin asymmetries. In particular, the final-state interactions from gluon exchange between the outgoing quark and the target spectator system lead to single-spin asymmetries in semi-inclusive deep inelastic lepton-proton scattering at leading twist in perturbative QCD; *i.e.*, the rescattering corrections of the struck quark with the target spectators are not power-law suppressed at large photon virtuality Q^2 at fixed x_{bj} [71] The final-state interaction from gluon exchange occurring immediately after the interaction of the current also produces a leading-twist diffractive component to deep inelastic scattering $\ell p \to \ell' p' X$ corresponding to color-singlet exchange with the target system; this in turn produces shadowing and anti-shadowing of the nuclear structure functions [67, 75]. In addition, one can show that the pomeron structure function derived from diffractive DIS has the same form as the quark contribution of the gluon structure function [74]. The final-state interactions occur at a short light-cone time $\Delta\tau \simeq 1/\nu$ after the virtual photon interacts with the struck quark, producing a non-trivial phase. Here $\nu = p \cdot q/M$ is the laboratory energy of the virtual photon. Thus none of the above phenomena is contained in the target light-front wave functions computed in isolation. In particular, the shadowing of nuclear structure functions is due to destructive interference effects from leading-twist diffraction of the virtual photon, physics not included in the nuclear light-front wave functions. Thus the structure functions measured in deep inelastic lepton scattering are affected by final-state rescattering, modifying their connection to light-front probability distributions. Some of these results can be understood by augmenting the light-front wave functions with a gauge link, but with a gauge potential created by an external field created by the virtual photon $q\bar{q}$ pair current [72]. The gauge link is also process dependent [73], so the resulting augmented LFWFs are not universal.

Single-spin asymmetries in hadronic reactions provide a remarkable window to QCD mechanisms at the amplitude level. In general, single-spin asymmetries measure the correlation of the spin projection of a hadron with a production or scattering plane [76]. Such correlations are odd under time reversal, and thus they can arise in a time-reversal invariant theory only when there is a phase difference between different spin amplitudes. Specifically, a nonzero correlation of the proton spin normal to a

production plane measures the phase difference between two amplitudes coupling the proton target with $J_p^z = \pm\frac{1}{2}$ to the same final-state. The calculation requires the overlap of target light-front wavefunctions with different orbital angular momentum: $\Delta L^z = 1$; thus a single-spin asymmetry (SSA) provides a direct measure of orbital angular momentum in the QCD bound state.

The observation that $\simeq 10\%$ of the positron-proton deep inelastic cross section at HERA is diffractive [77, 78] points to the importance of final-state gauge interactions as well as a new perspective to the nature of the hard pomeron. The same interactions are responsible for nuclear shadowing and Sivers-type single-spin asymmetries in semi-inclusive deep inelastic scattering and in Drell-Yan reactions. These new observations are in contradiction to parton model and light-cone gauge based arguments that final state interactions can be ignored at leading twist. The modifications of the deep inelastic lepton-proton cross section due to final state interactions are consistent with color-dipole based scattering models and imply that the traditional identification of structure functions with the quark probability distributions computed from the wavefunctions of the target hadron computed in isolation must be modified.

The shadowing and antishadowing of nuclear structure functions in the Gribov-Glauber picture is due to the destructive and constructive coherence, respectively, of amplitudes arising from the multiple-scattering of quarks in the nucleus. The effective quark-nucleon scattering amplitude includes Pomeron and Odderon contributions from multi-gluon exchange as well as Reggeon quark exchange contributions [75]. The multiscattering nuclear processes from Pomeron, Odderon and pseudoscalar Reggeon exchange leads to shadowing and antishadowing of the electromagnetic nuclear structure functions in agreement with measurements. An important conclusion is that antishadowing is nonuniversal—different for quarks and antiquarks and different for strange quarks versus light quarks. This picture thus leads to substantially different nuclear effects for charged and neutral currents, particularly in anti-neutrino reactions, thus affecting the extraction of the weak-mixing angle $\sin^2\theta_W$ and the constant ρ_o which are determined from the ratios of charged and neutral current contributions in deep inelastic neutrino and anti-neutrino scattering. In recent work, Schmidt, Yang, and I [79] find that a substantial part of the difference between the standard model prediction and the anomalous NuTeV result [80] for $\sin^2\theta_W$ could be due to the different behavior of nuclear antishadowing for charged and neutral currents. Detailed measurements of the nuclear dependence of charged, neutral and electromagnetic DIS processes are needed to establish the distinctive phenomenology of shadowing and antishadowing and to make the NuTeV results definitive.

5 Other QCD Phenomenology Related to Light-Front Wavefunctions

A number of important phenomenological properties follow directly from the structure of light-front wavefunctions in gauge theory.

(1). *Intrinsic Glue and Sea.* Even though QCD was motivated by the successes of the parton model, QCD predicts many new features which go well beyond the simple three-quark description of the proton. Since the number of Fock components cannot be limited in relativity and quantum mechanics, the nonperturbative wavefunction of a proton contains gluons and sea quarks, including heavy quarks at any resolution scale. Thus there is no scale Q_0 in deep inelastic lepton-proton scattering where the proton can be approximated by its valence quarks. Empirical evidence also continues to accumulate that the strange-antistrange quark distributions are not symmetric in the proton [81, 82].

(2) *Intrinsic Charm.* [83] The probability for Fock states of a light hadron such as the proton to have an extra heavy quark pair decreases as $1/m_Q^2$ in non-Abelian gauge theory [84, 85]. The relevant matrix element is the cube of the QCD field strength $G^3_{\mu\nu}$. This is in contrast to abelian gauge theory where the relevant operator is $F^4_{\mu\nu}$ and the probability of intrinsic heavy leptons in QED bound state is suppressed as $1/m_\ell^4$. The intrinsic Fock state probability is maximized at minimal off-shellness. It is useful to define the transverse mass $m_{\perp i} = \sqrt{k_{\perp i}^2 + m_i^2}$. The maximum probability then occurs at $x_i = m_\perp^i / \sum_{j=1}^n m_\perp^j$; *i.e.*, when the constituents have minimal invariant mass and equal rapidity. Thus the heaviest constituents have the highest momentum fractions and the highest x_i. Intrinsic charm thus predicts that the charm structure function has support at large x_{bj} in excess of DGLAP extrapolations [83]; this is in agreement with the EMC measurements [86]. It predicts leading charm hadron production and fast charmonium production in agreement with measurements [87]. In fact even double $J/\psi's$ are produced at large x_F, consistent with the dissociation and coalescence of double intrinsic Fock states of the projectile LFWF [88].

The proton wavefunction thus contains charm quarks with large light-cone momentum fractions x. The recent observation by the SELEX experiment [89, 90] showing that doubly-charmed baryons such as the Ξ_{cc}^+ and hence two charmed quarks are produced at large x_F and small p_T in hadron-nucleus collisions provides additional and compelling evidence for the diffractive dissociation of complex off-shell Fock states of the projectile. These observations contradict the traditional view that sea quarks and gluons are always produced perturbatively via DGLAP evolution. Intrinsic charm can also explain the $J/\psi \to \rho\pi$ puzzle [91]. It also affects the extraction of suppressed CKM matrix elements in B decays [92].

3. *Hidden Color.* A rigorous prediction of QCD is the "hidden color" of nuclear wavefunctions at short distances. QCD predicts that nuclear wavefunctions contain "hidden color" [93] components: color configurations not dual to the usual nucleonic

degrees of freedom. In general, the six-quark wavefunction of a deuteron is a mixture of five different color-singlet states [93]. The dominant color configuration at large distances corresponds to the usual proton-neutron bound state where transverse momenta are of order $\vec{k}^2 \sim 2M_d\epsilon_{BE}$. However, at small impact space separation, all five Fock color-singlet components eventually acquire equal weight, *i.e.*, the deuteron wavefunction evolves to 80% hidden color.

At high Q^2 the deuteron form factor is sensitive to wavefunction configurations where all six quarks overlap within an impact separation $b_{\perp i} < \mathcal{O}(1/Q)$. Since the deuteron form factor contains the probability amplitudes for the proton and neutron to scatter from $p/2$ to $p/2 + q/2$, it is natural to define the reduced deuteron form factor[94, 93]

$$f_d(Q^2) \equiv \frac{F_d(Q^2)}{F_{1N}\left(\frac{Q^2}{4}\right)\ F_{1N}\ \left(\frac{Q^2}{4}\right)}. \tag{7}$$

The effect of nucleon compositeness is removed from the reduced form factor. QCD then predicts the scaling

$$f_d(Q^2) \sim \frac{1}{Q^2}; \tag{8}$$

i.e., the same scaling law as a meson form factor. This scaling is consistent with experiment for $Q^2 > 1$ GeV^2. In fact as seen in Fig. 1, the deuteron reduced form factor contains two components: (1) a fast-falling component characteristic of nuclear binding with probability 85%, and (2) a hard contribution falling as a monopole with a scale of order 0.5 GeV with probability 15%. The normalization of the deuteron form factor observed at large Q^2 [95], as well as the presence of two mass scales in the scaling behavior of the reduced deuteron form factor [94] thus suggests sizable hidden-color Fock state contributions such as $|\,(uud)_{8_C}(ddu)_{8_C}\rangle$ with probability of order 15% in the deuteron wavefunction [96].

(4) *Color transparency.* The small transverse size fluctuations of a hadron wavefunction with a small color dipole moment will have minimal interactions in a nucleus [97, 98].

This has been verified in the case of diffractive dissociation of a high energy pion into dijets $\pi A \to q\bar{q}A'$ in which the nucleus is left in its ground state [99]. When the hadronic jets have balancing but high transverse momentum, one studies the small size fluctuation of the incident pion. The diffractive dissociation cross section is found to be proportional to A^2 in agreement with the color transparency prediction. Color transparency has also been observed in diffractive electroproduction of ρ mesons [100] and in quasi-elastic $pA \to pp(A-1)$ scattering [101] where only the small size fluctuations of the hadron wavefunction enters the hard exclusive scattering amplitude. In the latter case an anomaly occurs at $\sqrt{s} \simeq 5$ GeV, most likely signaling a resonance effect at the charm threshold [102].

Color transparency, as evidenced by the Fermilab measurements of diffractive dijet production, implies that a pion can interact coherently throughout a nucleus

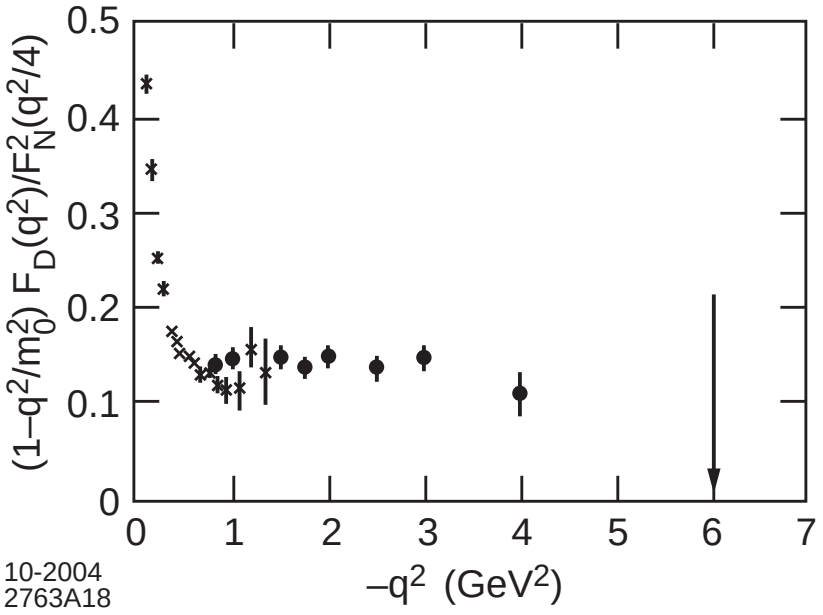

Figure 1: Reduced Deuteron Form Factor showing the scaling predicted by perturbative QCD and conformal scaling. The data show two regimes: a fast-falling behavior at small Q^2 characteristic of normal nuclear binding, and a hard scattering regime with monopole fall-off controlled by the scale $m_0^2 = 0.28$ GeV^2. The latter contribution is attributable to non-nucleonic hidden-color components of the deuteron's six-quark Fock state. From Ref. [94].

with minimal absorption, in dramatic contrast to traditional Glauber theory based on a fixed $\sigma_{\pi n}$ cross section. Color transparency gives direct validation of the gauge interactions of QCD.

6 Hard Exclusive Processes and Form Factors at High Q^2

Leading-twist PQCD predictions for hard exclusive amplitudes [54] are written in a factorized form as the product of hadron distribution amplitudes $\phi_I(x_i, Q)$ for each hadron I convoluted with the hard scattering amplitude T_H obtained by replacing each hadron with collinear on-shell quarks with light-front momentum fractions $x_i = k_i^+/P^+$. The hadron distribution amplitudes are obtained by integrating the $n-$parton valence light-front wavefunctions:

$$\phi(x_i, Q) = \int^Q \Pi_{i=1}^{n-1} d^2k_{\perp i}\ \psi_{\rm val}(x_i, k_\perp). \tag{9}$$

Thus the distribution amplitudes are $L_z = 0$ projections of the LF wavefunction, and the sum of the spin projections of the valence quarks must equal the J_z of the parent hadron. Higher orbital angular momentum components lead to power-law suppressed exclusive amplitudes [54, 39]. Since quark masses can be neglected at leading twist in T_H, one has quark helicity conservation, and thus, finally, hadron-helicity conservation: the sum of initial hadron helicities equals the sum of final helicities. In particular, since the hadron-helicity violating Pauli form factor is computed from states with $\Delta L_z = \pm 1$, PQCD predicts $F_2(Q^2)/F_1(Q^2) \sim 1/Q^2$ [modulo logarithms]. A detailed analysis shows that the asymptotic fall-off takes the form $F_2(Q^2)/F_1(Q^2) \sim \log^2 Q^2/Q^2$ [103]. One can also construct other models [9] incorporating the leading-twist perturbative QCD prediction which are consistent with the JLab polarization transfer data [104] for the ratio of proton Pauli and Dirac form factors. This analysis can also be extended to study the spin structure of scattering amplitudes at large transverse momentum and other processes which are dependent on the scaling and orbital angular momentum structure of light-front wavefunctions. Recently, Afanasev, Carlson, Chen, Vanderhaeghen, and I [105] have shown that the interfering two-photon exchange contribution to elastic electron-proton scattering, including inelastic intermediate states, can account for the discrepancy between Rosenbluth and Jefferson Lab spin transfer polarization data [104].

A crucial prediction of models for proton form factors is the relative phase of the timelike form factors, since this can be measured from the proton single spin symmetries in $e^+e^- \to p\bar{p}$ or $p\bar{p} \to \ell\bar{\ell}$ [106]. Carl Carlson, John Hiller, Dae Sung Hwang and I [106] have shown that measurements of the proton's polarization strongly discriminate between the analytic forms of models which fit the proton form factors in the spacelike region. In particular, the single-spin asymmetry normal to the scattering plane measures the relative phase difference between the timelike G_E and G_M form factors. The dependence on proton polarization in the timelike region is expected to be large in most models, of the order of several tens of percent. The continuation of the spacelike form factors to the timelike domain $t = s > 4M_p^2$ is very sensitive to the analytic form of the form factors; in particular it is very sensitive to the form of the PQCD predictions including the corrections to conformal scaling. The forward-backward $\ell^+\ell^-$ asymmetry can measure the interference of one-photon and two-photon contributions to $\bar{p}p \to \ell^+\ell^-$.

As discussed in section 2, dimensional counting rules for hard exclusive processes have now been derived in the context of nonperturbative QCD using the AdS/CFT correspondence. The data for virtually all measured hard scattering processes appear to be consistent with the conformal predictions of QCD. For example, recent measurements of the deuteron photodisintegration cross section $\gamma d \to pn$ follow the leading-twist s^{11} scaling behavior at large momentum transfers in the few GeV region [107, 108, 109]. This adds further evidence for the dominance of leading-twist quark-gluon subprocesses and the near conformal behavior of the QCD coupling. As discussed above, the evidence that the running coupling has constant fixed-point be-

havior, which together with BLM scale fixing, could help explain the near conformal scaling behavior of the fixed-CM angle cross sections. The angular distribution of hard exclusive processes is generally consistent with quark interchange, as predicted from large N_C considerations.

7 New Directions

As I have emphasized in this talk, the light-front wavefunctions of hadrons are the central elements of QCD phenomenology, describing bound states in terms of their fundamental quark and gluon degrees of freedom at the amplitude level. Given the light-front wavefunctions one can compute quark and gluon distributions, distribution amplitudes, generalized parton distributions, form factors, and matrix elements of local currents such as semileptonic B decays. The diffractive dissociation of hadrons on nucleons or nuclei into jets or leading hadrons provides new measures of the LFWFs of the projectile as well as tests of color transparency and intrinsic charm.

It is thus imperative to compute the light-front wavefunctions from first principles in QCD. Lattice gauge theory can provide moments of the distribution amplitudes by evaluating vacuum-to-hadron matrix elements of local operators [15]. The transverse lattice is also providing new nonperturbative information [13, 14].

The DLCQ method is also a first-principles method for solving nonperturbative QCD; at finite harmonic resolution K the DLCQ Hamiltonian acts in physical Minkowski space as a finite-dimensional Hermitian matrix in Fock space. The DLCQ Heisenberg equation is Lorentz-frame independent and has the advantage of providing not only the spectrum of hadrons, but also the complete set of LFWFs for each hadron eigenstate.

An important feature the light-front formalism is that J_z is conserved; thus one simplify the DLCQ method by projecting the full Fock space on states with specific angular momentum. As shown in ref. [9], the Karmanov-Smirnov operator uniquely specifies the form of the angular dependence of the light-front wavefunctions, allowing one to transform the light-front Hamiltonian equations to differential equations acting on scalar forms. A complementary method would be to construct the T-matrix for asymptotic $q\bar{q}$ or qqq or gluonium states using the light-front analog of the Lippmann-Schwinger method. This allows one to focus on states with the specific global quantum numbers and spin of a given hadron. The zeros of the resulting resolvent then provides the hadron spectrum and the respective light-front Fock state projections.

The AdS/CFT correspondence has now provided important new information on the short-distance structure of hadronic LFWFs; one obtains conformal constraints which are not dependent on perturbation theory. The large $k_\perp$ fall-off of the valence LFWFs is also rigorously determined by consistency with the evolution equations for the hadron distribution amplitudes [54]. Similarly, one can also use the structure of the evolution equations to constrain the $x \to 1$ endpoint behavior of the LFWFs. One can use these strong constraints on the large $k_\perp$ and $x \to 1$ behavior to model

the LFWFs. Such forms can also be used as the initial approximations to the wavefunctions needed for variational methods which minimize the expectation value of the light-front Hamiltonian.

Acknowledgments

I wish to thank Professors Ben Bakker, Piet Mulders, and their colleagues at the Vrije Universiteit in Amsterdam for hosting this outstanding meeting. This talk is based on collaborations with Guy de Teramond, Markus Diehl, Rikard Enberg, John Hiller, Paul Hoyer, Dae Sung Hwang, Gunnar Ingelman, Volodya Karmanov, Gary McCartor, Sven Menke, Carlos Merino, Joerg Raufeisen, and Johan Rathsman.

References

[1] P. A. M. Dirac, Rev. Mod. Phys. **21**, 392 (1949).

[2] S. J. Brodsky, H. C. Pauli and S. S. Pinsky, Phys. Rept. **301**, 299 (1998) [arXiv:hep-ph/9705477].

[3] P. P. Srivastava and S. J. Brodsky, Phys. Rev. D **64**, 045006 (2001) [arXiv:hep-ph/0011372].

[4] P. P. Srivastava and S. J. Brodsky, Phys. Rev. D **66**, 045019 (2002) [arXiv:hep-ph/0202141].

[5] R. L. Jaffe and A. Manohar, Nucl. Phys. B **337**, 509 (1990).

[6] X. D. Ji, Nucl. Phys. Proc. Suppl. **119**, 41 (2003) [arXiv:hep-lat/0211016].

[7] S. J. Brodsky and S. D. Drell, Phys. Rev. D **22**, 2236 (1980).

[8] J. Carbonell, B. Desplanques, V. A. Karmanov, and J. F. Mathiot, Phys. Rep. **300**, 215 (1998) [arXiv:nucl-th/9804029].

[9] S. J. Brodsky, J. R. Hiller, D. S. Hwang and V. A. Karmanov, Phys. Rev. D **69**, 076001 (2004) [arXiv:hep-ph/0311218].

[10] V. A. Karmanov and A.V. Smirnov, Nucl. Phys. A **546**, 691 (1992).

[11] H. C. Pauli and S. J. Brodsky, Phys. Rev. D **32**, 2001 (1985).

[12] W. A. Bardeen, R. B. Pearson and E. Rabinovici, Phys. Rev. D **21**, 1037 (1980).

[13] S. Dalley, arXiv:hep-ph/0409139.

[14] M. Burkardt and S. Dalley, Prog. Part. Nucl. Phys. **48**, 317 (2002) [arXiv:hep-ph/0112007].

[15] L. Del Debbio, M. Di Pierro, A. Dougall and C. T. Sachrajda [UKQCD collaboration], Nucl. Phys. Proc. Suppl. **83**, 235 (2000) [arXiv:hep-lat/9909147].

[16] P. Maris and C. D. Roberts, Int. J. Mod. Phys. E **12**, 297 (2003) [arXiv:nucl-th/0301049].

[17] D. J. Gross, A. Hashimoto and I. R. Klebanov, Phys. Rev. D **57**, 6420 (1998) [arXiv:hep-th/9710240].

[18] K. Hornbostel, S. J. Brodsky and H. C. Pauli, Phys. Rev. D **41**, 3814 (1990).

[19] M. Harada, J. R. Hiller, S. Pinsky and N. Salwen, Phys. Rev. D **70**, 045015 (2004) [arXiv:hep-th/0404123].

[20] S. J. Brodsky, J. R. Hiller and G. McCartor, Annals Phys. **305**, 266 (2003) [arXiv:hep-th/0209028].

[21] M. van Iersel and B. L. G. Bakker, arXiv:hep-ph/0407318. B. L. G. Bakker, M. van Iersel, and F. Pijlman, Few-Body Systems **33**, 27 (2003).

[22] H. C. Pauli, arXiv:hep-ph/0312300.

[23] M. Weinstein, arXiv:hep-th/0410113.

[24] H. Zhan, A. Nogga, B. R. Barrett, J. P. Vary and P. Navratil, Phys. Rev. C **69**, 034302 (2004) [arXiv:nucl-th/0401047].

[25] S. Dalley, Nucl. Phys. B (Proc. Suppl.) **108**, 145 (2002).

[26] S. J. Brodsky, Published in *Nagoya 2002, Strong coupling gauge theories and effective field theories, 1-18.* [arXiv:hep-th/0304106].

[27] F. Antonuccio, S. J. Brodsky and S. Dalley, Phys. Lett. B **412**, 104 (1997) [arXiv:hep-ph/9705413].

[28] J. M. Maldacena, Adv. Theor. Math. Phys. **2**, 231 (1998) [Int. J. Theor. Phys. **38**, 1113 (1999)] [arXiv:hep-th/9711200].

[29] J. Polchinski and M. J. Strassler, Phys. Rev. Lett. **88**, 031601 (2002) [arXiv:hep-th/0109174].

[30] R. C. Brower and C. I. Tan, Nucl. Phys. B **662**, 393 (2003) [arXiv:hep-th/0207144].

[31] O. Andreev, Phys. Rev. D **67**, 046001 (2003) [arXiv:hep-th/0209256].

[32] S. J. Brodsky and G. R. Farrar, Phys. Rev. Lett. **31**, 1153 (1973).

[33] V. A. Matveev, R. M. Muradian and A. N. Tavkhelidze, Lett. Nuovo Cim. **7**, 719 (1973).

[34] S. J. Brodsky and G. R. Farrar, Phys. Rev. D **11**, 1309 (1975).

[35] S. J. Brodsky, Published in *Newport News 2002, Exclusive processes at high momentum transfer 1-33.* [arXiv:hep-ph/0208158.]

[36] S. J. Brodsky, M. Burkardt and I. Schmidt, Nucl. Phys. B **441**, 197 (1995) [arXiv:hep-ph/9401328].

[37] S. J. Rey and J. T. Yee, Eur. Phys. J. C **22**, 379 (2001) [arXiv:hep-th/9803001].

[38] S. J. Brodsky and G. F. de Teramond, Phys. Lett. B **582**, 211 (2004) [arXiv:hep-th/0310227].

[39] X. d. Ji, J. P. Ma and F. Yuan, Phys. Rev. Lett. **90**, 241601 (2003) [arXiv:hep-ph/0301141].

[40] S. J. Brodsky, SLAC-PUB-10206 *Invited talk at International Conference on Color Confinement and Hadrons in Quantum Chromodynamics - Confinement 2003, Wako, Japan, 21-24 Jul 2003*

[41] G. Parisi, Phys. Lett. B **39**, 643 (1972).

[42] S. J. Brodsky, Y. Frishman, G. P. Lepage and C. Sachrajda, Phys. Lett. **91B**, 239 (1980).

[43] S. J. Brodsky, P. Damgaard, Y. Frishman and G. P. Lepage, Phys. Rev. D **33**, 1881 (1986).

[44] S. J. Brodsky, Y. Frishman and G. P. Lepage, Phys. Lett. B **167**, 347 (1986).

[45] V. M. Braun, G. P. Korchemsky and D. Muller, Prog. Part. Nucl. Phys. **51**, 311 (2003) [arXiv:hep-ph/0306057].

[46] G. P. Lepage and S. J. Brodsky, Phys. Lett. B **87**, 359 (1979).

[47] S. J. Brodsky and G. P. Lepage, SLAC-PUB-4947 *In *A.H. Mueller, (ed): Perturbative Quantum Chromodynamics, 1989, p. 93-240,* and S. J. Brodsky, SLAC-PUB-8649 *In *Shifman, M. (ed.): At the frontier of particle physics, Handbook of QCD: Boris Ioffe Festschrift, vol. 2*, 2001, p 1343-1444.*

[48] S. J. Brodsky and H. J. Lu, Phys. Rev. D **51**, 3652 (1995) [arXiv:hep-ph/9405218].

[49] S. J. Brodsky, E. Gardi, G. Grunberg and J. Rathsman, Phys. Rev. D **63**, 094017 (2001) [arXiv:hep-ph/0002065].

[50] S. J. Brodsky, G. T. Gabadadze, A. L. Kataev and H. J. Lu, Phys. Lett. **B372**, 133 (1996) [arXiv:hep-ph/9512367].

[51] S. J. Brodsky, G. P. Lepage and P. B. Mackenzie, Phys. Rev. D **28**, 228 (1983).

[52] S. J. Brodsky, C. R. Ji, A. Pang and D. G. Robertson, Phys. Rev. D **57**, 245 (1998) [arXiv:hep-ph/9705221].

[53] S. J. Brodsky, S. Menke, C. Merino and J. Rathsman, Phys. Rev. D **67**, 055008 (2003) [arXiv:hep-ph/0212078].

[54] G. P. Lepage and S. J. Brodsky, Phys. Rev. D **22**, 2157 (1980).

[55] L. von Smekal, R. Alkofer and A. Hauck, Phys. Rev. Lett. **79**, 3591 (1997) [arXiv:hep-ph/9705242].

[56] D. Zwanziger, Phys. Rev. D **69**, 016002 (2004) [arXiv:hep-ph/0303028].

[57] D. M. Howe and C. J. Maxwell, Phys. Lett. B **541**, 129 (2002) [arXiv:hep-ph/0204036].

[58] D. M. Howe and C. J. Maxwell, Phys. Rev. D **70**, 014002 (2004) [arXiv:hep-ph/0303163].

[59] S. Furui and H. Nakajima, arXiv:hep-lat/0309166.

[60] A. C. Mattingly and P. M. Stevenson, Phys. Rev. D **49**, 437 (1994) [arXiv:hep-ph/9307266].

[61] M. Baldicchi and G. M. Prosperi, Phys. Rev. D **66**, 074008 (2002) [arXiv:hep-ph/0202172].

[62] K. Ackerstaff *et al.* [OPAL Collaboration], Eur. Phys. J. C **7**, 571 (1999) [arXiv:hep-ex/9808019].

[63] B. Melic, B. Nizic and K. Passek, Phys. Rev. D **65**, 053020 (2002) [arXiv:hep-ph/0107295].

[64] S. J. Brodsky and D. S. Hwang, Nucl. Phys. B **543**, 239 (1999) [arXiv:hep-ph/9806358].

[65] S. J. Brodsky, D. S. Hwang, B. Q. Ma and I. Schmidt, Nucl. Phys. B **593**, 311 (2001) [arXiv:hep-th/0003082].

[66] S. J. Brodsky, M. Diehl and D. S. Hwang, Nucl. Phys. B **596**, 99 (2001) [arXiv:hep-ph/0009254].

[67] S. J. Brodsky, P. Hoyer, N. Marchal, S. Peigne and F. Sannino, Phys. Rev. D **65**, 114025 (2002) [arXiv:hep-ph/0104291].

[68] J. Raufeisen and S. J. Brodsky, arXiv:hep-th/0408108.

[69] J. D. Bjorken, Phys. Rev. **179**, 1547 (1969).

[70] E. D. Bloom *et al.*, Phys. Rev. Lett. **23**, 930 (1969).

[71] S. J. Brodsky, D. S. Hwang and I. Schmidt, Phys. Lett. B **530**, 99 (2002) [arXiv:hep-ph/0201296].

[72] A. V. Belitsky, X. Ji and F. Yuan, Nucl. Phys. B **656**, 165 (2003) [arXiv:hep-ph/0208038].

[73] J. C. Collins, Phys. Lett. B **536**, 43 (2002) [arXiv:hep-ph/0204004].

[74] S. J. Brodsky, R. Enberg, P. Hoyer and G. Ingelman, arXiv:hep-ph/0409119.

[75] S. J. Brodsky and H. J. Lu, Phys. Rev. Lett. **64**, 1342 (1990).

[76] D. W. Sivers, Phys. Rev. D **43**, 261 (1991).

[77] M. Derrick *et al.* [ZEUS Collaboration], Phys. Lett. B **315**, 481 (1993).

[78] T. Ahmed *et al.* [H1 Collaboration], Nucl. Phys. B **429**, 477 (1994).

[79] S. J. Brodsky, I. Schmidt and J. J. Yang, arXiv:hep-ph/0409279.

[80] G. P. Zeller *et al.* [NuTeV Collaboration], Phys. Rev. Lett. **88**, 091802 (2002) [Erratum-ibid. **90**, 239902 (2003)] [arXiv:hep-ex/0110059].

[81] S. J. Brodsky and B. Q. Ma, Phys. Lett. B **381**, 317 (1996) [arXiv:hep-ph/9604393].

[82] S. Kretzer, arXiv:hep-ph/0408287.

[83] S. J. Brodsky, P. Hoyer, C. Peterson and N. Sakai, Phys. Lett. B **93**, 451 (1980).

[84] M. Franz, V. Polyakov and K. Goeke, Phys. Rev. D **62**, 074024 (2000) [arXiv:hep-ph/0002240].

[85] S. J. Brodsky, J. C. Collins, S. D. Ellis, J. F. Gunion and A. H. Mueller, DOE/ER/40048-21 P4 *Proc. of 1984 Summer Study on the SSC, Snowmass, CO, Jun 23 - Jul 13, 1984*

[86] B. W. Harris, J. Smith and R. Vogt, Nucl. Phys. B **461**, 181 (1996) [arXiv:hep-ph/9508403].

[87] J. C. Anjos, J. Magnin and G. Herrera, Phys. Lett. B **523**, 29 (2001) [arXiv:hep-ph/0109185].

[88] R. Vogt and S. J. Brodsky, Phys. Lett. B **349**, 569 (1995) [arXiv:hep-ph/9503206].

[89] A. Ocherashvili *et al.* [SELEX Collaboration], arXiv:hep-ex/0406033.

[90] M. Mattson *et al.* [SELEX Collaboration], Phys. Rev. Lett. **89**, 112001 (2002) [arXiv:hep-ex/0208014].

[91] S. J. Brodsky and M. Karliner, Phys. Rev. Lett. **78**, 4682 (1997) [arXiv:hep-ph/9704379].

[92] S. J. Brodsky and S. Gardner, Phys. Rev. D **65**, 054016 (2002) [arXiv:hep-ph/0108121].

[93] S. J. Brodsky, C. R. Ji and G. P. Lepage, Phys. Rev. Lett. **51**, 83 (1983).

[94] S. J. Brodsky and B. T. Chertok, Phys. Rev. D **14**, 3003 (1976).

[95] R. G. Arnold *et al.*, Phys. Rev. Lett. **35**, 776 (1975).

[96] G. R. Farrar, K. Huleihel and H. y. Zhang, Phys. Rev. Lett. **74**, 650 (1995).

[97] G. Bertsch, S. J. Brodsky, A. S. Goldhaber and J. F. Gunion, Phys. Rev. Lett. **47**, 297 (1981).

[98] S. J. Brodsky and A. H. Mueller, Phys. Lett. B **206**, 685 (1988).

[99] D. Ashery, Comments Nucl. Part. Phys. **2**, A235 (2002).

[100] A. B. Borisov [HERMES Collaboration], Nucl. Phys. A **711**, 269 (2002).

[101] J. Aclander *et al.*, arXiv:nucl-ex/0405025.

[102] S. J. Brodsky and G. F. de Teramond, Phys. Rev. Lett. **60**, 1924 (1988).

[103] A. V. Belitsky, X. D. Ji and F. Yuan, Phys. Rev. Lett. **91**, 092003 (2003) [arXiv:hep-ph/0212351].

[104] M. K. Jones *et al.* [Jefferson Lab Hall A Collaboration], Phys. Rev. Lett. **84**, 1398 (2000) [arXiv:nucl-ex/9910005].

[105] Y. C. Chen, A. Afanasev, S. J. Brodsky, C. E. Carlson and M. Vanderhaeghen, arXiv:hep-ph/0403058.

[106] S. J. Brodsky, C. E. Carlson, J. R. Hiller and D. S. Hwang, Phys. Rev. D **69**, 054022 (2004) [arXiv:hep-ph/0310277].

[107] R. J. Holt, Phys. Rev. **C41**, 2400 (1990).

[108] C. Bochna *et al.* [E89-012 Collaboration], Phys. Rev. Lett. **81**, 4576 (1998) [arXiv:nucl-ex/9808001].

[109] P. Rossi *et al.* [CLAS Collaboration], arXiv:hep-ph/0405207.